NASA

Technical Memorandum **85097**

FLUID SIGNATURES OF ROTATIONAL DISCONTINUITIES AT THE EARTH'S MAGNETOPAUSE

Jack D. Scudder

September 1983

National Aeronautics and
Space Administration

Goddard Space Flight Center
Greenbelt, Maryland 20771

FLUID SIGNATURES OF ROTATIONAL DISCONTINUITIES AT THE EARTH'S MAGNETOPAUSE

by

Jack D. Scudder
NASA/Goddard Space Flight Center
Laboratory for Extraterrestrial Physics
Greenbelt, MD 20771

SUBMITTED TO: Journal of Geophysical Research

ABSTRACT

Fluid signatures in the MHD approximation at rotational discontinuities (RD) of finite width called rotational shear layers (RSL) are examined for general flow and magnetic geometries. This is necessary to obtain an overview of the fluid signatures of RSL's as well as their frequency of occurrence at general locations on a curved magnetopause. RSL's at the magnetopause are necessary for the MHD description of an open magnetosphere. Analytical and geometrical arguments illustrate that the fluid speed can either go up or down across an RSL for a fixed normal mass flux. The speed profile may or may not be monotonic depending on the boundary conditions. The flow velocity may or may not be field aligned or "jetting" ($\hat{V}\cdot\hat{B} \approx 1$) as a result of traversing the RSL. In general, significant "convection" is expected in the layer. The observable signatures of (MHD) RSL's depend on 7 (boundary condition) parameters: (1) the mass density, (2-5): the incident normal and transverse components of the magnetic field and fluid velocity, (6): the angle ε between the incident tangential flow velocity and tangential magnetic field, and (7): the size of the magnetic angular rotation implemented by the layer $\Delta\phi$. The geometry Petschek, Levy and Siscoe (PLS) have considered is a special case of this general study when the tangential fluid velocity vanishes and the magnetic rotation is maximal. This general survey illustrates the singular character of the PLS geometry and that the predictions of "jetting" and monotonic speed increases through the layer may <u>not</u> be used as general signatures of RSL's at general places along the magnetopause where the fluid flow, $\Delta\phi$ and ε are generally all different from the PLS regime. Accordingly, the lack of observed speed increases across the magnetopause can no longer be used by itself to infer that the magnetopause is locally closed. Of the spectrum of MHD RSL's that are possible the "accelerating" ones require special boundary conditions most generally occurring near the nose of the magnetopause; the "decelerating" RSL's become increasingly more probable at magnetopause crossings removed from the sub-solar point. Documented RSL's have been located within the spectrum of possible signatures; the rareness of reported RSL's is attributed to an overly narrow view of their definitive signatures.

1. INTRODUCTION

For many years searches have been conducted at the earth's magnetopause to determine the topological nature of the boundary--whether it was open or closed. The question was initially investigated with high resolution magnetic field data; the approach attempted to determine whether the temporal records provided by spaceborne magnetometers were consistent with having traversed a rotational or tangential discontinuity (Sonnerup and Cahill 1968, Sonnerup and Ledley 1974, 1979). These tests were motivated by the theoretical model of Levy et al. (1964) which requires rotational discontinuity surfaces to stand at the magnetopause on either side of the reconnector/separator line. Penetration of these surfaces was considered more likely than traversals of the reconnection line. The existence of rotational discontinuities at the magnetopause would permit directed normal mass fluxes to enter an "open" magnetosphere without the benefit of diffusion mechanisms. The difficulties in identifying rotational discontinuities (RD's) from magnetic records alone is well known; however, this method did find some defensible RD magnetopause crossings. In recent years plasma, magnetic and electric field data have been examined to answer this fundamental question about the nature of the interface between the earth's magnetic cavity and the magnetosheath. In a survey of two years of ISEE data Paschmann et al. (1979) and Sonnerup et al. (1981) reported the detection of 12 magnetopause crossings that were consistent with RD signatures of the reconnection models of Levy et al. (1964). These events occurred primarily near the nose of the magnetopause and had speed increases across them. Recently, Aggson et al. (1983a) have confirmed the rotational character of the Sonnerup et al. (1981) events using electric and magnetic field data. Using this same technique Aggson et al. (1983b) have also reported a rotational magnetopause traversal in which the observed fluid speed decreased; they pointed out that this behavior was permitted for the geometrical circumstances encountered under the MHD description of RD's as outlined, for example, by de Hoffman and Teller (1950) and mentioned by Roederer (1977).

It is a well known property (Walén, 1944) for a rotational discontinuity (RD), rotational shear layer (RSL), or a sharply crested finite amplitude Alfvén wave that the fluctuation vector of the fluid, $\Delta\underline{V}$, is proportional to

the fluctuation vector of the magnetic field, $\Delta \underline{B}$,

$$\Delta \underline{V} = \alpha \Delta \underline{B}. \qquad (1)$$

The constant of proportionality is defined as $\alpha = V_N/B_N$ where V_N and B_N are the normal flow velocity and magnetic field in the frame of the RD. This is a deceptively simple relationship. Because (1) is a vector difference equation it is difficult to foresee the general relationship between the directly observable velocity and magnetic field that its quadrature permits in the presence of shear layers that satisfy (1).

If the curved magnetopause were generally an RSL the plasma velocity on the magnetosheath side of the RSL would be oblique to the normal of the RSL. This geometry is significantly different from the situation at the nose where the sheath flow velocity is very nearly along the RSL normal as assumed in the Levy et al. model. In the past it has been tacitly assumed that the signatures of an RSL away from the nose do not differ significantly from those expected at the nose where the Levy et al. model predicts field aligned speed enhancements relative to the magnetosheath across relational discontinuities (RSL's) standing in the flow on either side of the separator. The absence of these signatures led Heikkila (1975) to question the importance of reconnection at the magnetopause. On the basis of these unfulfilled expectations it has been concluded by Haerendel et al. (1978) that large portions of the magnetopause are "closed" to the direct normal mass flux permitted by an RD/RSL. The properties of an RSL for general incident flows tangential to the magnetopause must be explored before we can confidently outline the expected plasma signatures of an RSL at an arbitrary position along the magnetopause and accept Haerendel et al's. conclusion.

In addition, the maximal rotation of the magnetic field ($\phi = \pi$) assumed in the Levy et al. model can only occur at restricted locations on the magnetopause as outlined by Crooker (1979). Contrary to the assumption of Levy et al. (1964), even these locales will always have substantial tangential sheath velocities, $\underline{V}_T$; RSL signatures for finite V_T should be anticipated there. If RSL's are present at other places on the magnetopause we must expect the more general signatures that accompany $\phi < \pi$ and $V_T > 0$.

In this paper the general fluid signatures for a rotational shear layer with assumed isotropic pressure are examined. We assume these layers are locally planar and of sufficient thickness to ignore finite Larmor corrections to MHD which are necessary for very thin layers. This approach is similar in spirit to the level of tests described by Sonnerup et al. (1981). Of interest are: 1) the characteristic signatures of RSL's if resolved in the fluid flow in terms of characteristic angles between $\underline{B}$ and $\underline{V}$ through the layer, 2) the speed profiles that are compatible with traversing a rotational shear layer, and 3) the physical parameters that determine the RSL characteristics. Does, for example, a decrease in the fluid speed contradict the rotational character (i.e. openess) of the layer? Must the speed profile by monotonic? Is jetting a diagnostic of an RSL? What would be the signatures of a partial passage in and out of a shear layer? Are flux transfer events (FTE's, Russell and Elphic (1979)) compatible with such behavior?

2. GEOMETRICAL CONSTRUCTIONS

If a time stationary locally planar shear layer is rotational then the normal components of the magnetic field and flow, B_N and V_N, respectively, as well as the mass density ρ are non-zero and conserved under the assumption of isotropic pressure. Further $V_N = \pm B_N/\sqrt{4\pi\rho}$. Equation 1 in this geometry merely restates the boundary condition that the electric field tangential to the wave front is conserved through the layer. The geometric content of (1) is that the changes to the initial $\underline{B}^o$ and $\underline{V}^o$ are always parallel or anti-parallel through the layer. Given the conserved quantities, equation (1) is equivalent to a similar relationship between the transverse components (subscript T) of $\underline{B}$ and $\underline{V}$ which are perpendicular to the wave normal:

$$\Delta\underline{V}_T = \alpha\Delta\underline{B}_T. \qquad (2)$$

Equation (2) applies only to planar RSL's, since the general MHD result (1) admits solutions that are <u>not</u> rotations confined to a plane (cf. Whang 1973, Goldstein et al. 1974, Barnes and Hollweg (1974) and Behannon and Burlaga 1978 (1981)).

It is well known in an isotropic plasma that $\alpha = \pm 1/\sqrt{4\pi\rho}$. If we absorb the modulus of alpha into a newly defined vector $\underline{\beta}$ defined by

$$\underline{\beta} \equiv \frac{1}{\sqrt{4\pi\rho}} \underline{B}, \tag{3}$$

which has the units of velocity, the magnetic and velocity changes of equation (2) may be examined graphically in terms of the equivalent statement

$$\Delta \underline{V}_T = \pm \Delta \underline{\beta}_T. \tag{3b}$$

All of the essential geometry of equations (2) or (3b) can be viewed in the plane perpendicular to the normal, $\hat{n}$. In Figure 1 the general content of this relation is constructed as follows. The incident $\underline{\beta}_T^o$ is placed along the X axis, OA; a semi-circle ABD (dotted) is constructed with $\underline{\beta}_T^o$ on a bounding diameter (the sense of the polarization of the rotation starting at $\underline{\beta}_T^o$ is dictated by either electrons (for $B_N<0$ clockwise-downward) or protons (for $B_N<0$ counter clockwise-upward). According to Sonnerup and Cahill (1968) the electron polarization, adopted here, appears to be preferred at the earth's magnetopause. From the origin the vector $\underline{V}_T^o$ defined by

$$\underline{V}_T^o \equiv \underline{V} \cdot (\underline{\underline{I}} - \hat{n}\hat{n}) = \underline{V} - (\underline{V} \cdot \hat{n})\hat{n},$$

is constructed which is generally non-zero at the magnetopause and oriented at a counter-clockwise angle $\varepsilon = \sin^{-1}[(\hat{\underline{\beta}}_T^o \times \hat{\underline{V}}_T^o) \cdot \hat{n}]$ to $\underline{\beta}_T^o$. Through $\underline{V}_T^o$ is constructed a line A'D' parallel to $\underline{\beta}_T^o$. A portion of this line is used as a diameter of another semi-circle A'B'D' of radius $|\underline{\beta}_T^o|$ with its center at O' displaced opposite to (along) $\hat{\underline{\beta}}_T^o$ by a distance $|\underline{\beta}_T^o|$ and having the same (or opposite) concavity depending on whether $\Delta \underline{V}$ is $+(-)\Delta\underline{\beta}$ in equation (3b). $\underline{V}_T^o$ is related to the frame velocity $\underline{U}^o$ necessary to achieve the de Hoffman-Teller (1950) description ($\underline{E} = 0$)of the rotation exploited by Aggson et al. (1983a,b) by the relation $\underline{U}^o = \underline{V}_T^o - R_N\underline{\beta}_T^o = \underline{V}^o - R_N\underline{\beta}^o$, where $R_N \equiv V_N/(B_N\sqrt{4\pi\rho})$ which is ± 1 for an RSL. For clarity the $\underline{U}^o$ vector has been omitted but would be given by the ray OO' in Figures 1-3. By this construction all chords $\Delta\underline{V}_T^i(\Delta\underline{\beta}_T^i)$ passing through $\underline{\beta}_T^o, (\underline{V}_T^o)$ subtend equal angles of the respective semi-circles, are either parallel (anti-parallel) and of equal length, and thus implement equations 1, 3b.

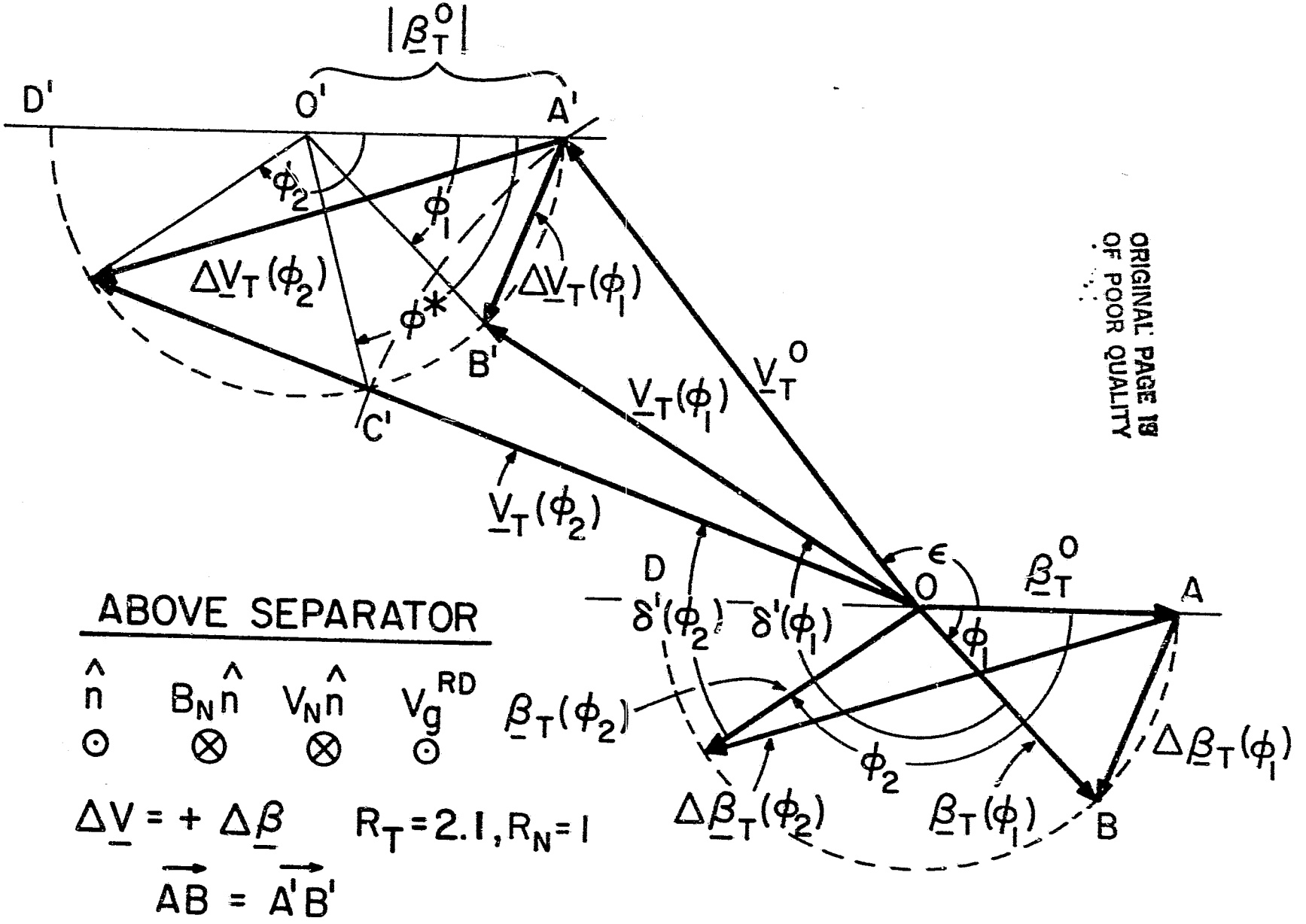

Figure 1

The concrete example of Figure 1 illustrates the important dimensionless variables that affect the geometry and the signature of an RSL in the general situation: the magnetic rotation angle ϕ, the angle ε between $\underline{B}_T^o$ and $\underline{V}_T^o$, and the ratio of speeds defined as $R_T \equiv |\underline{V}_T^o|/|\underline{B}_T^o|$. Physically, this ratio is very nearly the Alfven Mach number of the tangential flow provided $|B_N| << |\underline{B}_T|$. We loosely refer to this ratio as the "tangential Mach number". If the magnetic rotation $\Delta\phi$ is not maximal (π), consider $\phi=\phi_1<\phi^*$, for the choice of ε and R_T of Figure 1 the fluid speed will go down across an RSL in the presence of a normal mass flux. We will show below that this non-monotonic speed property with angle ϕ is a general property of $R_T \neq 0$ RSL's.

Figure 2 illustrates the same type construction but with R_T exactly zero, which corresponds to the usually studied normal incident geometry of Levy et al. (1964) and Petschek (1966). In this example, $\Delta\underline{V}_T(\phi) \equiv \underline{V}_T(\phi)$ and it is clear that, for any finite magnetic rotation, the fluid speed increases. Also clear from this construction is that $\underline{V}_T(\pi)$ is parallel to $\underline{B}_T(\pi)$, a property often referred to as "jetting." We will show below that this speed and jetting behavior represents a singular regime in parameter space when R_T is precisely zero, the rotation is maximal and the layers have zero thickness. We will show below that if R_T is non-zero there always exists ε,ϕ combinations for which the speed jump across the RSL is negative. To prove this assertion we need some analysis.

3. ANALYSIS

To achieve a general predictive capability of an RSL in general flow geometry we define a cartesian system in the plane orthogonal to the current sheet normal. There is no loss in generality to place the incident scaled transverse magnetic vector, $\underline{B}_T^o$, along the x axis and $\underline{V}_T^o$ displaced in a counter-clockwise manner to it by an angle ε about the (sheath sensed) magnetopause normal $\hat{n}$, which is taken as the z axis. Assuming a local one-dimensional shear layer, all the functions depend on z only. Therefore, the magnetic and flow fields may be written as

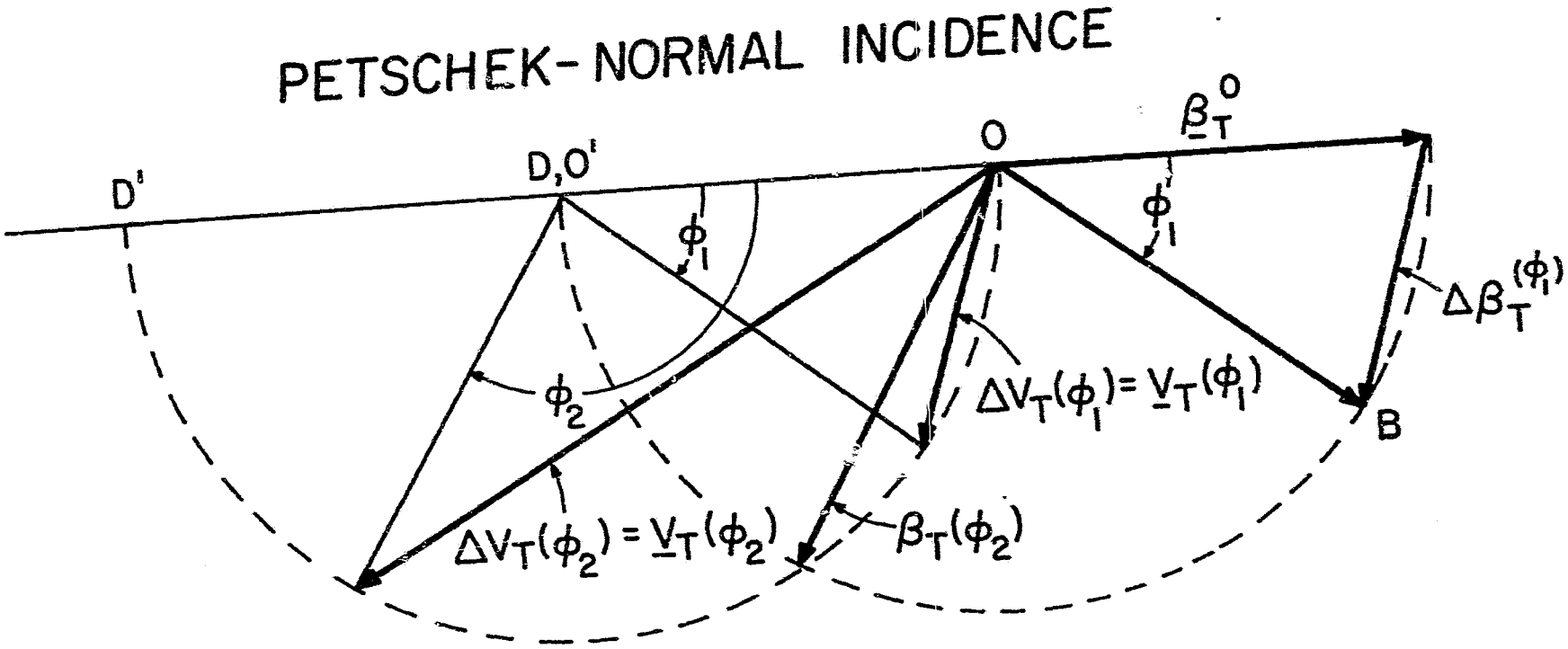

$\hat{n}$ $B_N\hat{n}$ $V_N\hat{n}$ V_g^{RD}

⊙ ⊗ ⊗ ⊙

$R_T = 0, R_N = 1$

Figure 2

$$\underline{B}(z) = \begin{pmatrix} B_T^{\,o} \cos\phi(z) \\ B_T^{\,o} \sin\phi(z) \\ B_z \end{pmatrix} \qquad \underline{V}(z) = \begin{pmatrix} V_T^{\,o} \cos\varepsilon + \Delta V_x(z) \\ V_T^{\,o} \sin\varepsilon + \Delta V_y(z) \\ V_z \end{pmatrix}$$

while the initial vectors outside the shear layer prior to traversal of the rotation of $\underline{B}$ are given by

$$\underline{B}^o = \begin{pmatrix} B_T^{\,o} \\ 0 \\ B_N \end{pmatrix} \qquad \text{and} \qquad \underline{V}^o = \begin{pmatrix} V_T^{\,o} \cos\varepsilon \\ V_T^{\,o} \sin\varepsilon \\ V_N \end{pmatrix}$$

where $B_N \equiv B\cdot\hat{n}$; $V_N = \underline{V}^o\cdot\hat{n}$; $B_T = |\underline{B}_T|$; $\underline{B}_T = (\underline{\underline{I}}-\hat{n}\hat{n})\cdot B$; $\underline{V}_T^{\,o} = (\underline{\underline{I}}-\hat{n}\hat{n})\cdot\underline{V}^o$; and $V_T^{\,o} = |\underline{V}_T^{\,o}|$.

The scaled speed ratio ν is defined as $|\underline{V}(\phi)|/|\underline{V}(\phi=0)|$. Its functional dependence on ε, ϕ, R_T, R_N, and γ can easily be shown to be

$$\nu(\varepsilon,\phi,R_T,R_N,\gamma) = \left[\frac{R_T^{\,2}+2R_NR_T\{\cos(\varepsilon-\phi)-\cos\varepsilon\} + R_N^{\,2}(2-2\cos\phi+\gamma^2)}{R_T^{\,2}+\gamma^2R_N^{\,2}}\right]^{1/2}, \qquad (4)$$

where $\gamma \equiv B_N^{\,o}/B_T^{\,o}$, $R_T = V_T^{\,o}/(B_T^{\,o}/\sqrt{4\pi\rho})$, $R_N = V_N^{\,o}/(B_N^{\,o}/\sqrt{4\pi\rho})$ and ε is the included angle between $\hat{B}_T^{\,o}$ and $\hat{V}_T^{\,o}$ defined by a right-handed coordinate system with $\hat{z}$ along the outward pointing magnetopause normal, and ϕ is the signed sense of rotation of $\hat{B}_T$, being positive for counter-clockwise rotations looking down on magnetopause from the sheath. The angle $\delta(\phi)$ defined by

$$\delta(\phi) = \cos^{-1}\left(\hat{V}(\phi)\cdot\hat{B}(\phi)\right)$$

can also be reduced to its essential functional dependence in the form of

$$\delta(\varepsilon,\phi,R_T,R_N,\gamma) = \cos^{-1}\left[\frac{R_T\cos(\varepsilon-\phi)+R_N(1-\cos\phi+\gamma^2)}{(1+\gamma^2)^{1/2}(R_T^{\,2}+2R_NR_T\{\cos(\varepsilon-\phi)-\cos\varepsilon\}+R_N^{\,2}(2-2\cos\phi+\gamma^2))^{1/2}}\right]. \qquad (5)$$

Neither (4) nor (5) is very transparent except in the normal incidence limit ($R_T\to 0$) or infinite Mach number regime $R_T \to \infty$.

In the normal incidence limit they become

$$\nu(\varepsilon,\phi,0,R_N,\gamma) = \frac{(2-2\cos\phi+\gamma^2)^{1/2}}{\gamma} \tag{6a}$$

and

$$\delta(\varepsilon,\phi,0,R_N,\gamma) = \cos^{-1}\frac{(1-\cos\phi+\gamma^2)R_N/|R_N|}{(1+\gamma^2)^{1/2}(2-2\cos\phi+\gamma^2)^{1/2}} \tag{7a}$$

Equation 6a shows that at normal incidence the speed ratio increases monotonically with $\phi \leq \pi$ and inversely with normal B_N strength. In the Levy et al. regime of $\phi = \pi$ (7a) reduces to $\delta = \cos^{-1}[R_N/(|R_N|/(1+\gamma^2/4)^{1/2}]$ which implies $\delta(\gamma \to 0) = (1 - R_N/|R_N|)\pi/2$, which is the "jetting" behavior. Because the argument of the arc cosine never vanishes equation 7a implies that δ can never be $\pi/2$. Accordingly, pure plasma convection ($\delta = \pi/2$) is not present in an RSL at strict normal incidence.

In the infinite tangential Mach number limit (6a) and (7a) become

$$\nu(\varepsilon,\phi,R_T\to\infty, R_N, \gamma) = 1 \tag{6b}$$

and

$$\delta(\varepsilon,\phi,R_T\to\infty,R_n,\gamma) = \cos^{-1}(\cos(\varepsilon-\phi)/\{1+\gamma^2\}^{1/2}), \tag{7b}$$

which in the limit of small magnetic normal component approaches

$$\nu(\varepsilon,\phi\ R_T\to\infty, R_N, \gamma\to 0) = 1 \tag{6c}$$

$$\delta(\varepsilon,\phi,R_T\to\infty, R_N, \gamma\to 0) = \varepsilon - \phi. \tag{7c}$$

These asymptotic trends should be compared with graphical presentations below in Figures 4F, L, 6F,L for equations (6a), (7a) and Figures 4A,C, 6A,C for equations (6b), (7b).

4. GRAPHICAL SUMMARY OF RSL MORPHOLOGY FOR $|\gamma|^{-1} = 20\sqrt{2}$

To explore the more general behavior of equations (4) and (5) as functions of 5 variables we have assumed a single value for $\gamma = B_N^o/B_T^o = 1/(20\sqrt{2})$, noted that R_N can only take on the discrete values of ± 1, have examined a spectrum of 6 values of $R_T = \{0.01, 0.1, 0.5, 1., 1.5, 10\}$ for all possible values of ε and ϕ. Depending on the actual value of B_T^o, γ determines the B_N^o value being considered; B_N^o together with the mass density and the value of R_N determine the V_N^o being discussed. Similarly the choice of B_T^o and ρ, together with the value of R_T determines the actual values of tangential flow being considered. Exploring (4) and (5) at even this depth requires 24 isocontours (Figures 4,6). Our purpose is to illustrate the diversity of the possible RSL signatures that would be anticipated for fixed γ rather than to provide an exhaustive glossary of the content of (4), (5), which are general and can be adapted to γ regimes not selected here.

Following the results of Sonnerup and Cahill (1968), we consider only the electron polarization of the RD, namely, that $\hat{B}_T$ rotates according to the right-hand rule if the thumb is placed along $B_N\hat{n}$. Since by (1)

$$\Delta \underline{V} = \frac{V_N}{B_N} \Delta \underline{B},$$

and since above (below) the separator at the earth's magnetopause B_N <(>) 0 and V_N <(<) 0, $\Delta\underline{V}$ and $\Delta\underline{B}$ are parallel (antiparallel) above (below) the separator as B_T rotates through $\Delta\phi = \phi_{max}$ (cf. Figure 3a,b). This implies that $R_N = -\dot{\phi}/|\dot{\phi}|$. To the extent that V_T/V_N and B_T/B_N are large numbers the angle δ between $\underline{V}$ and $\underline{B}$ through the layer is nearly the angle $\delta'(\phi) = \cos^{-1}(\hat{V}_T(\phi)\cdot\hat{B}_T(\phi))$ indicated in Figure 3.

In Figure 4(A-L) we consider the spectrum of possible speed ratios, v, that would be seen across a rotational discontinuity standing in the flow (as at the magnetopause) as a function of R_T, ε, ϕ_{max} and R_N with γ fixed). The left column corresponds to $R_N = -1$ and would apply to an RSL encounter below

ROTATIONAL DISCONTINUITIES STANDING IN FLOW
(ELECTRON POLARIZATION)

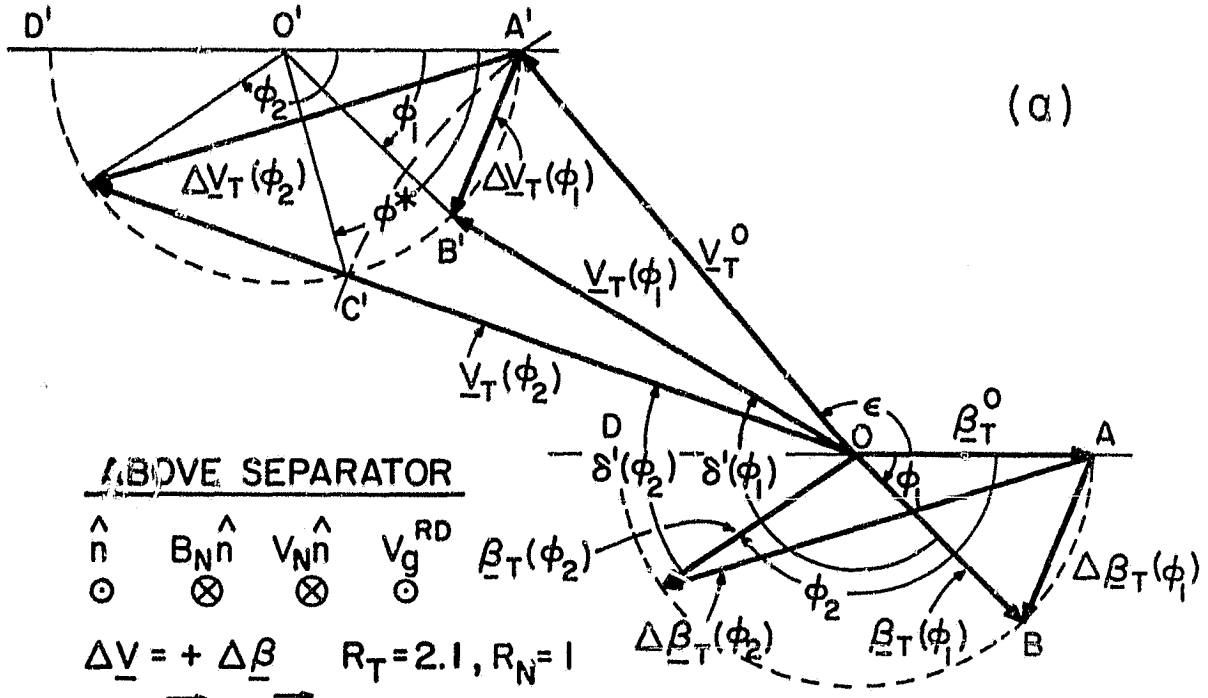

ABOVE SEPARATOR

$\hat{n}$	$B_N\hat{n}$	$V_N\hat{n}$	V_g^{RD}
⊙	⊗	⊗	⊙

$\Delta \underline{V} = + \Delta \underline{\beta}$ $\quad R_T = 2.1, R_N = 1$

$\overrightarrow{AB} = \overrightarrow{A'B'}$

$$R_N = -\dot{\phi} / |\dot{\phi}|$$

(b)

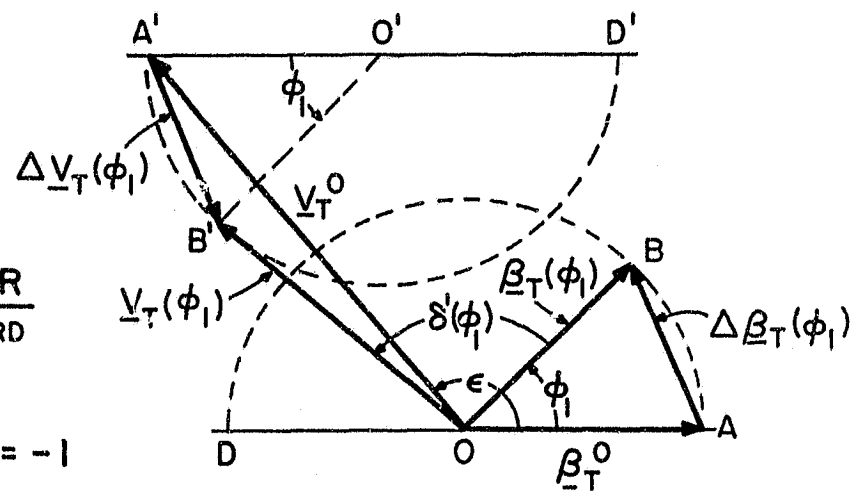

BELOW SEPARATOR

$\hat{n}$	$B_N\hat{n}$	$V_N\hat{n}$	V_g^{RD}
⊙	⊙	⊗	⊙

$R_T = 2.1, R_N = -1$

$\Delta \underline{V} = -\Delta \underline{\beta}$

$\overrightarrow{AB} = -\overrightarrow{A'B'}$

Figure 3

the magnetic separator; the right column corresponds to $R_N = +1$ and being above the separator. Each row of boxes is for a fixed value of R_T indicated in the central portion of the figure with the horizontal axis of each graph being the angle of magnetic rotation ($0 < \phi_{max} < \pi$) and the vertical axis being the angle ε between $\hat{B}_T^o$ and $\hat{V}_T^o$ as viewed from the sheath side of the magnetopause which ranges between $(0,2\pi)$. From the top the six separate graphs in each column correspond to decreasing tangential Mach numbers (10, 1.5, 1.0, 0.5, 0.1, 0.01) of the incident flow.

Every finite tangential Mach number regime of Figure 4 contains dynamo regions ($\nu<1$) (of varying size) in which the RD decreases the incident flow speed relative to the magnetosheath. The larger the tangential Mach number, R_T, the larger the dynamo region. The largest percentage decreases in scaled plasma speed, ν, are accomplished for $R_T \sim 1$ flows and are preferentially located below $\varepsilon = \pi$. As normal incidence is approached the dynamo region has vanishing area, consistent with equation (6a). Notice as $R_T > 1$ that there are even RSL regimes with maximal magnetic rotation (ϕ,π) across which the fluid speed will still decrease significantly (cf. Figure 4B,H).

The speed ratios are most dramatic (notice change in contour labels!) for low tangential Mach numbers which approximate the Petschek normal incidence geometry. However, because the incident flows are so weak in this regime, large speed ratios, ν, need not imply large flow speeds in an absolute sense. At hyper-Alfvénic tangential flows (Figure 4A,G) (such as on the flanks of the magnetopause or in typical solar wind geometries, Burlaga et al. (1977)) the speed contrasts become very small whether or not motor- or dynamo like behavior is present.

The transition between $\nu>1$ and $\nu<1$ is the boundary between motor and dynamo behavior of the RSL. The conserved tangential electric field is given by

$$\underline{E}_T = 1/c \begin{pmatrix} -V_T^o \sin\varepsilon\, B_N \\ V_T^o \cos\varepsilon\, B_N - B_T V_N \\ 0 \end{pmatrix}$$

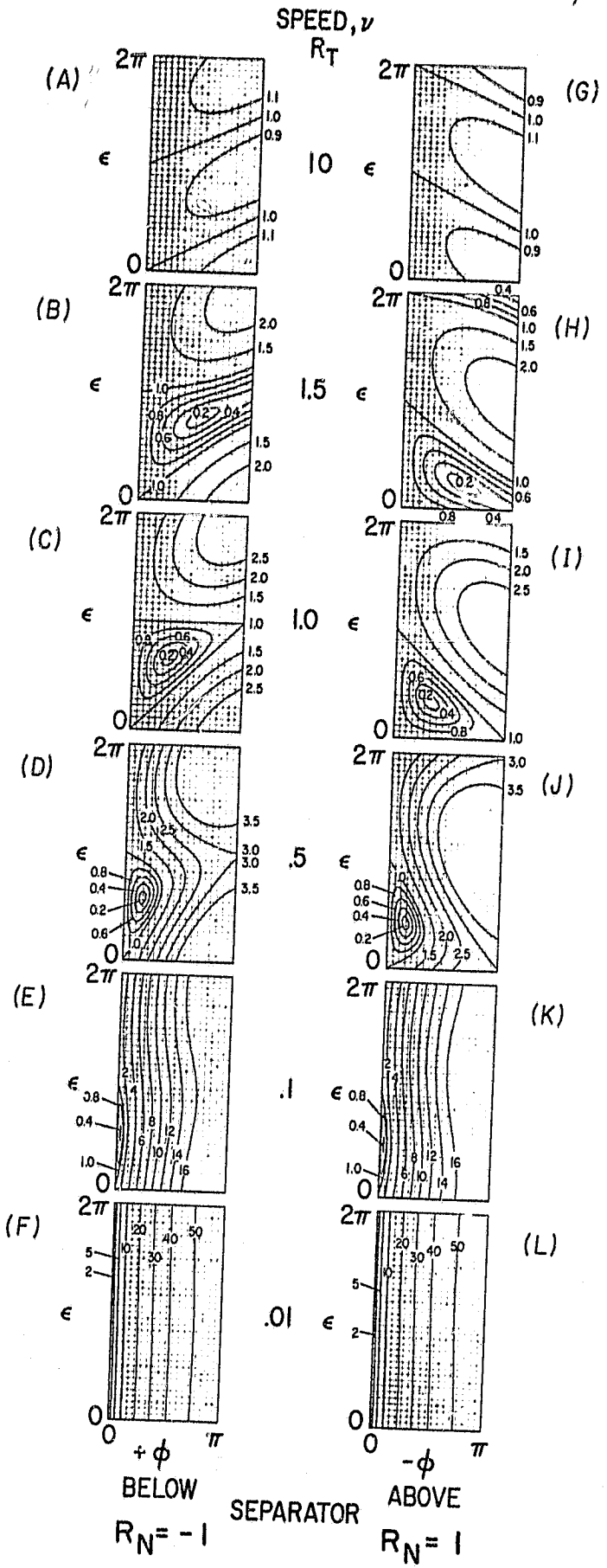

Figure 4

The current density is given by

$$\underline{J} = c/4\pi \begin{pmatrix} -dB_y/dz \\ dB_x/dz \\ 0 \end{pmatrix} = \frac{cB_T}{4\pi} \begin{pmatrix} -\cos\phi \; d\phi/dz \\ -\sin\phi \; d\phi/dz \\ 0 \end{pmatrix}$$

and the energy per square centimeter per second available to the fluid as a result of traversing the RSL with angular shear of ϕ_{max} is given by

$$\Delta\underline{E}\cdot\underline{J} = \frac{-1}{4\pi} B_T^2 V_n \{\frac{R_T}{R_N} \sin\varepsilon \sin\phi_{max} + (\frac{R_T}{R_N} \cos\varepsilon - 1)(\cos\phi_{max} - 1)\}. \qquad (8)$$

For the normal incidence geometry ($R_T \to 0$) of Levy et al. (1964) $\Delta \underline{E}\cdot\underline{J}$ reduces to

$$\lim_{R_T \to 0} \Delta \underline{E}\cdot\underline{J} = -1/4\pi \; B_T^2 \; V_n \; (1 - \cos\phi_{max}) \qquad (9)$$

which is positive definite for $0 < \phi_{max} < 2\pi$ (recall that $V_n < 0$). By being positive definite regardless of ϕ_{max} this result implies that the fluid on traversing the rotational layer (at normal incidence) is strictly energized at the expense of the electromagnetic field (cf. Figure 4F,L and discussion and equation (6a)). This behavior is often referred to as "motor-like." The opposite behavior is often referred to as "dynamo-like."

Figure 5 (left and right) synthesizes Figure 4 left and right columns by superimposing the $\Delta E\cdot J = 0$ ($v_o = 1$) contours of equation (8) of the different R_T regimes onto one figure. The curves have been labeled by their R_T value. The shaded regions indicate certain ε, ϕ_{max} angle combinations that only permit "motor"-like transitions regardless of the tangential Mach number. The compliment to these regions contains varying subdomains of "dynamo"-like layers with sizes that depend on the tangential Mach number.

The sign of $\Delta\underline{E}\cdot\underline{J}$ determines whether net work has been given to or extracted from the fluid in traversing the rotational discontinuity. It is, therefore, interesting to identify the conditions, if physical, when $\Delta\underline{E}\cdot\underline{J}$ changes sign. From equation (8) it is clear that the leading coefficients are

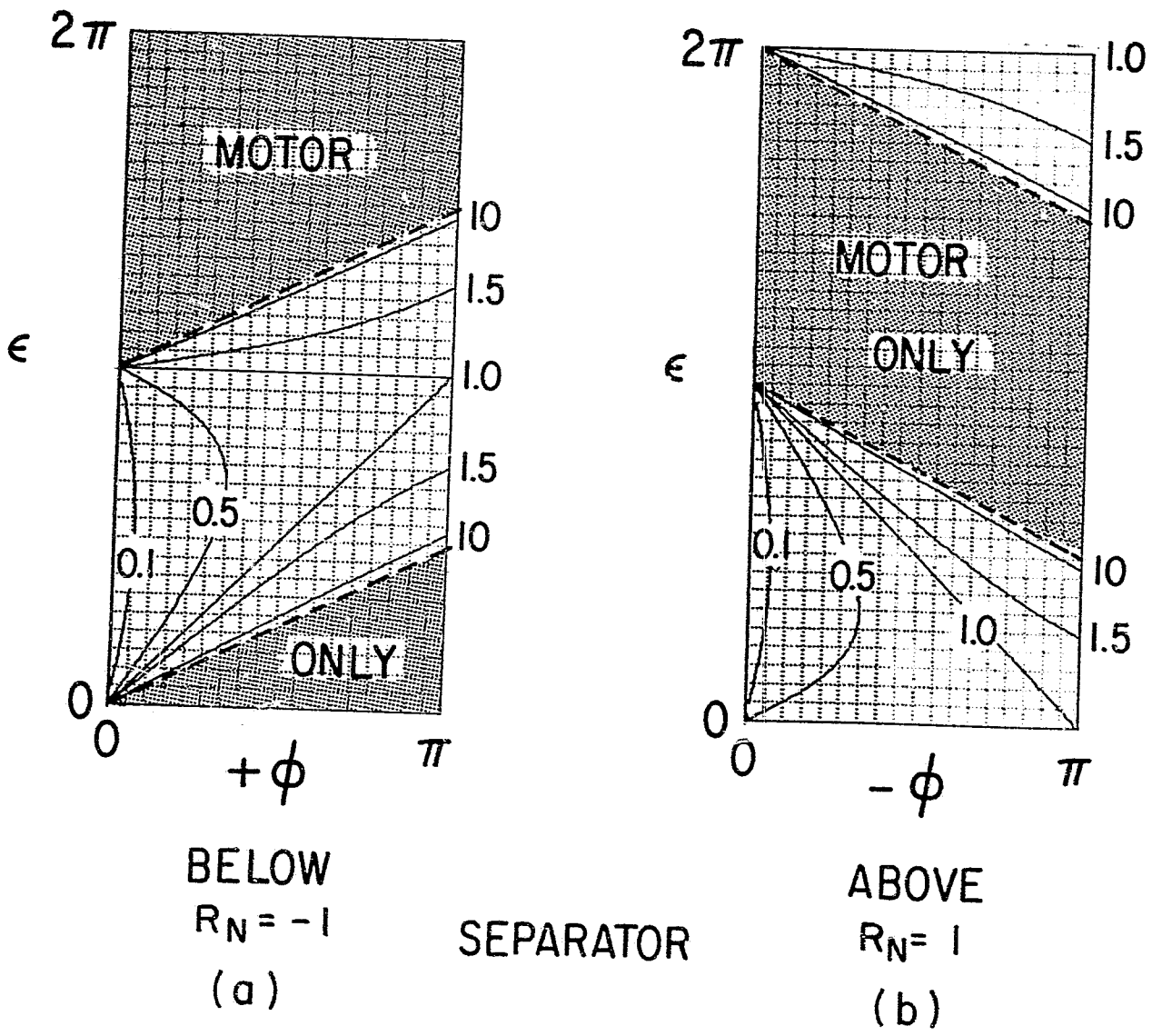

Figure 5

non-zero, if the layer remains rotational. The work done changes sign when the term in parentheses changes sign. This transition takes place for the ratio R_T^o, such that

$$R_T^o(\Delta \underline{E}\cdot\underline{J} = 0, \phi_{max}, \varepsilon) = \frac{R_N\,(\cos\phi_{max}-1)}{(\cos(\phi_{max}-\varepsilon)-\cos\varepsilon)}. \qquad (10)$$

Equation (10) shows that R_T^o will flip sign at the poles of this expression. This condition implies that on either side of

$$\varepsilon = \phi_{max}/2 + (0,\pi)$$

there will be a transition between motor and dynamo behavior for the same sense of mass flux. These boundaries in the ε, ϕ space are indicated with heavy dotted lines and all dynamo-motor transitions for finite R_T do not cross these dotted lines. The shaded regions of Figure 5 denote the ε-ϕ domain where RSL's are always motor-like regardless of tangential Mach number, R_T. Outside the shaded regions motor-dynamo behavior depends on R_T.

This important result shows that for a general ε there are some ranges of angles of the magnetic rotation which depend on R_T for which the layer speeds up the plasma, and there are complimentary ranges which implement a slowing down of the plasma, while still permitting a constant sense of mass flux across the layer.

Figure 6 shows the variation of the angle δ between $\hat{V}(\phi)$ and $\hat{B}(\phi)$ as a function of ε and of $\phi = \phi_{max}$ of the magnetic rotation in the same format as Figure 4. For low tangential Mach numbers the RD quickly reorients the full velocity vector in a monotonic way toward being quasi-anti-parallel (below the separator) and quasi-parallel (above the separator) - regardless of the initial ε angle as implied by (7a). This "jetting" tendency is not general for different tangential Mach numbers nor for arbitrary magnetic rotations. In the hyper-Alfvênic domain the perturbation $\Delta\underline{V}_T$ cannot significantly alter $\hat{V}(\phi)$ from its value at ϕ=0. Therefore the angle $\delta(\phi, R_T{}^{+\infty})$ approaches (cf. equation 7c)

$$\delta(\phi, R_T{}^{+\infty}) \underline{\sim} \varepsilon - \phi,$$

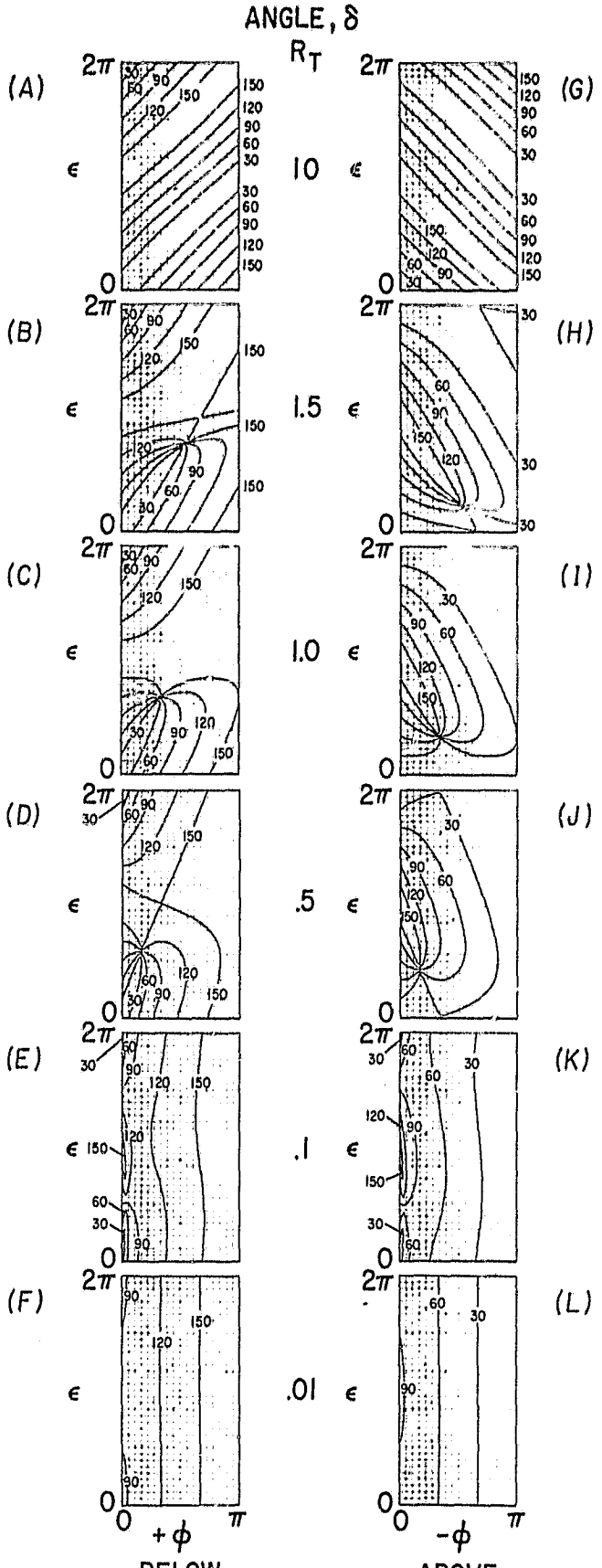

Figure 6

which says that the contour of constant $\delta = x^o$, is given by

$$\varepsilon = x^o - (-\phi) \quad \text{Above Separator.}$$
$$= x^o + \phi \quad \text{Below}$$

which closely resembles the curves in Figures 6A,G which clearly do not show jetting even for $\phi_{max} = \pi$.

By contrast the trans-Alfvénic cases illustrate that the angle δ can be a non-monotonic function of ϕ, the magnetic rotation, particularly for $\varepsilon<\pi$. Note that "jetting", while a property of $\phi_{max}\to\pi$ for $R_T \lesssim 1$, is not a general signature of traversal of an RD for which the magnetic rotation is not maximal. In addition, if the RSL is resolved, significant convective electric fields will be present because $0<\delta(\phi)<\pi$ until $\phi\to\pi$, consistent with the measurements reported by Aggson et al. (1983a). Surveys keying on the presence of "jetting" are biased against the more general RD's of submaximal angular rotations, especially in the presence of finite R_T.

The regions of these graphs associated with southward IMF in the forward magnetopause are regions with $\phi<\phi_{max}>>\pi/2$. If the separator is localized near the nose then $\varepsilon\sim\pi\pm\Delta$ above the separator and $\varepsilon\sim 0\pm\Delta$ below the separator. If flux transfer events are partial passes through an RD magnetopause layer (Scudder et al. (1983)) the observed angular excursion ϕ^{obs}_{max} in $\underline{B}_T$ is by definition less than the total ϕ^{MP}_{max} of the entire traversal of the magnetopause. Therefore if the IMF is southward by the angle ψ then

$$\phi < \phi^{obs}_{max} < \phi^{MPS}_{max} \lesssim \pi/2 + \psi$$

If, on the other hand ϕ^{obs}_{max} must be "significant" in order to define the events (Russell and Elphic 1979) ϕ^{obs}_{max} should not be small either. Therefore, FTE's

as a class (if they are partial RD traversals) must pertain to the regime $0 < \phi \lesssim \pi/2+\psi$. By virtue of the flow geometry and ε requirements it is clear that there is a broad regime of convection ($\delta \sim \pi/2$) near $\phi \lesssim 5\pi/6$ below the separator (and near $\varepsilon \lesssim \pi/6$ above the separator) towards $\phi_{max} \gtrsim \pi/2$.

As the tangential Mach number approaches the normal incidence limit the isocontours of Figure 6F, and 6L become increasingly vertical (independent of ε). This is in accord with equation (7a). Notice that the sequence of $R_T \neq 0$ in Figure 6 shows the decreasing probability of encountering $\delta \sim \pi/2$ for general rotations, consistent with vanishing probability of pure convection at normal incidence argued from equation (7a).

By construction of Figure 6 either: (1) the angle $|\phi|$ may be interpreted as the internal structure of a given rotational layer with total magnetic rotation $|\phi_{max}| > \phi$; or (2), these diagrams can be looked at as restating the jump conditions across different RD's for given R_T, ε, ϕ in the graphs. In the first view the existence of "motor→ dynamo" transitions at ϕ_0 ($0 < \phi_0 < \pi$ for fixed ε, R_T) implies that the speed through the layer as scaled by the initial speed is unity at both $\phi=0$, $\phi=\phi_0$; the scaled speed is therefore non-monotonic with increasing magnetic rotation. For $R_T \lesssim 1$ the dynamo region precedes the motor regime with increasing magnitude of the angle of magnetic rotation. Above R_T the motor or dynamo regime may occur first cf. figure 4(b) $\varepsilon \sim 0$, $\varepsilon \gtrsim \pi$. Depending on the total magnitude of the magnetic rotation $|\phi_{max}|$, the initial ε, and R_T the speed profile at an RSL can, in general, increase or decrease monotonically with ϕ, or have net increases or decreases with non-monotonic speed profiles through the layer, or not change at all (cf. Figure 4C).

5. SUMMARY AND IMPLICATIONS

5.1 General RSL's

A general analysis has been performed for planar rotational shear layers (RSL) (broad rotational discontinuities) in the MHD (isotropic pressure) approximation to determine what variations of the flow speed and direction are expected through them. Analytic and graphical results imply that these

variations depend on: 1) the ratio γ of normal to tangential magnetic field strengths in the layer (B_N^o/B_T^o); 2) the transverse Alfvén Mach number, R_T defined by $|\underline{V}_T^o|/(B_T^o|/\sqrt{4\pi\rho})$, where V_T^o is the incident transverse flow velocity and ρ is the fluid mass density); 3) the incident angle ε between $\hat{B}_T^o$ and $\hat{V}_T^o$; 4) the magnitude and sense of the magnetic rotation, $\Delta\phi$, implemented by the layer; as well as 5) the location of the observer relative to the separator which defines the sign of R_N. These general results show that the total plasma fluid speed may either go up, down or even remain the same as a result of traversing the RSL depending on the initial conditions ε and R_T and the boundary conditions in the form of $\Delta\phi$. It has also been shown that the speed profile through the RSL need not even be monotonic when viewed as a function of the magnetic angle of rotation, ϕ. Simple geometric constructions have been presented to corroborate the analysis.

The Levy-Petschek-Siscoe normal incidence model of reconnection requires an RSL, assumed to be a rotational discontinuity (characterized by $R_T=0$ and $\Delta\phi=\pi$) in the MHD flow surrounding the reconnecting line. The general analysis presented above shows that "jetting" and large speed increases at the rotational layer, which are properties of the Petschek geometry, are not universal properties of these layers, but specialized properties for $\Delta\phi=\pi$, and $R_T<1$. If the magnetic rotation is less than 180^o, jetting is less prominent. As the transverse Mach number increases the percentage speed change across an RSL gets smaller and the likelihood that the rotation implements a net speed decrease increases. Speed decreases are most likely when $0<\varepsilon<\pi$ and $\Delta\phi << \pi/2$ for $R_T<1$, but this domain can extend over the regime $\pi/2<\varepsilon<3\pi/2$ as R_T increases as shown in Figure 4B,H. Conversely, speed increases and jetting are the expected signatures for all ε when $\Delta\phi > \pi/2$ and $R_T \leq 1$ (cf. Figures 4D,E,F,J,K,L, 6D,E,F,J,K,L).

Away from the nose of the magnetopause when $R_T\neq 0$ there exist appreciable ε, $\Delta\phi$ regimes where the signatures of RSL's allow the speed to decrease; in these locales Petschek's geometry is too specialized for its predictions to be observable even if an RSL were traversed.

5.2 Implications for Entry/Boundary Layers

Accordingly, fluid speed decreases across the magnetopause boundary or substantial convection within the boundary must no longer be considered as valid arguments against the rotational ("open") nature of the magnetopause. The survey of the HEOS data of the low latitude boundary layer by Paschmann et al. (1976) and Haerendel et al. (1978) need not imply that these regions are necessarily closed, since the principal evidence set forth for this interpretation was that the speed always decreased across the magnetopause. However, Eastman and Hones (1979) concluded that the electron microstates reveal both open and closed signatures at different energies.

The speed decreases across the magnetopause reported by the HEOS and IMP surveys have been previously used to exclude coherent normal mass flux as the source of the boundary layers sampled, these data are the extant experimental evidence for various variants of diffusive mass and momentum entry into the magnetosphere. Since speed decreases are possible results of an RSL with a directed normal mass flux, the entire question of the observational evidence for a closed magnetosphere must be completely reexamined. It is possible that the extant data are consistent with the magnetopause being an RSL everywhere with spatially varying mass fluxes, which, if small, make the local magnetopause appear degenerate with, but not topologically equivalent to, a tangential discontinuity. In this circumstance the similarities of the plasma boundary layer and magnetosheath plasma distribution functions would naturally result from the magnetic connection of the two regimes.

5.3 Implications for Reported RSL Magnetopause Crossings

Thirteen RSL's have been reported at the earth's magnetopause using ISEE data. Twelve of the episodes had speed increases (Paschmann et al. (1979), Sonnerup et al. (1981) and Gosling et al. (1982)); recently an RSL with a net speed decrease has been documented by Aggson et al. (1983b). To date no systematic search has been conducted to determine the relative frequency of occurrence or location of these two classes of RSL's; the Paschman-Sonnerup-Gosling (PSG) events have all keyed on the speed increase to define events (Paschmann, 1983 private communication).

Figure 7 illustrates the distribution of the above cited RSL's in terms of the observed tangential Alfvén Mach number, R_T, of the magnetosheath flow which plays a pivotal role in the RSL ν profile. All of the speed increase events of PSG occur with $R_T < 1.1$ with a mean of $0.5 \pm {}^{.6}_{.5}$. The Aggson et al. event in which the speed decreased occurred at a much higher tangential Mach number (2.8) than any of the PSG events. Figure 8 illustrates the angular location of these events relative to noon; this graph together with Figure 7 illustrates that $R_T < 1$ clearly orders the conditions of PSG $\nu > 1$ events better than does subsolar angular location. When the solar wind/magnetosheath Alfvén Mach number is very low the tangential Mach number, R_T, can be quite low at appreciable angular distances from the nose as in the Gosling et al. event. Under more typical solar wind conditions the angular location of the Gosling events would ordinarily correspond to $R_T >> 1$ such as seen in the Aggson et al. event. This spectrum of behavior is expected on the basis of Figure 4 especially when it is recalled that most of these events have $\Delta\phi \lesssim 180°$ so that the ε dependence for $R_T < 1$ events does not seriously compromise the high expectation of $\nu > 1$. As can be seen in Figure 4 the precise magnitude of ν even in this regime depends on ε. Also expected in this regime is that ν is larger for smaller R_T. The minimum value of the PS events was 0.3 and it produced $\nu \backsim 4.5$; the Gosling et al. event had $R_T \backsim 0.04$–0.08 and $\nu = 2$–3 whereas the largest R_T of Sonnerup (1.1) gave the smallest $\nu = 1.3$ of the events with full data presented.

The deceleration event of August 12, 1978, reported by Aggson et al. (1983) occurred at $\backsim 70°$ of the subsolar point with dimensionless boundary conditions of $R_T = 2.8$, $\varepsilon = 25°$ and $-\Delta\phi \backsim 165°$, which were estimated from ambient data assuming $\underline{B}_T \backsim \underline{B}$; $\underline{V}_T \backsim \underline{V}$. Figure 9 illustrates ν contours for $\gamma_*^{-1} \equiv B_T/B_N = -20$ $\sqrt{2}$ for an RSL crossing above the separator. The choice of γ_* for Figures 4,5,9 is consistent with the geometrical upper bound on γ possible at a rotational discontinuity with $\measuredangle\, \underline{B}, \underline{B}_2 < 175°$, given by

$$\gamma < \sqrt{(1 + \cos\psi)/1 - \cos\psi)}$$

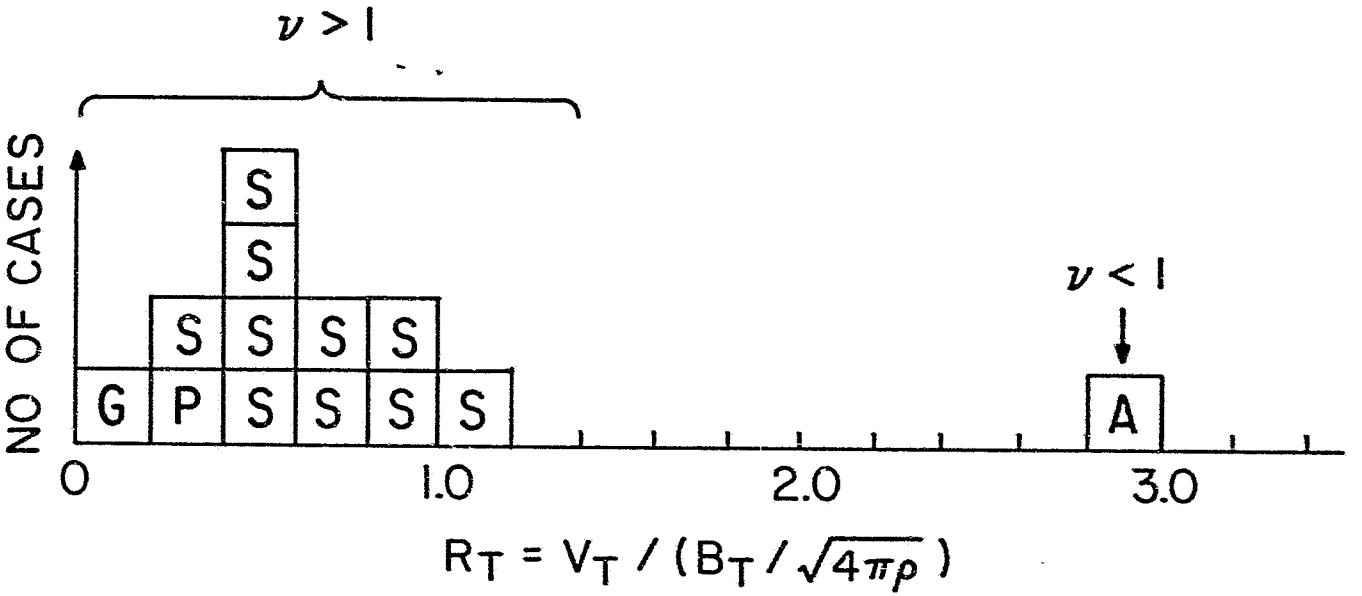

Figure 7

P-PASCHMANN ET AL (1979)

S-SONNERUP ET AL (1981)

G-GOSLING ET AL (1982)

A-AGGSON ET AL (1983b)

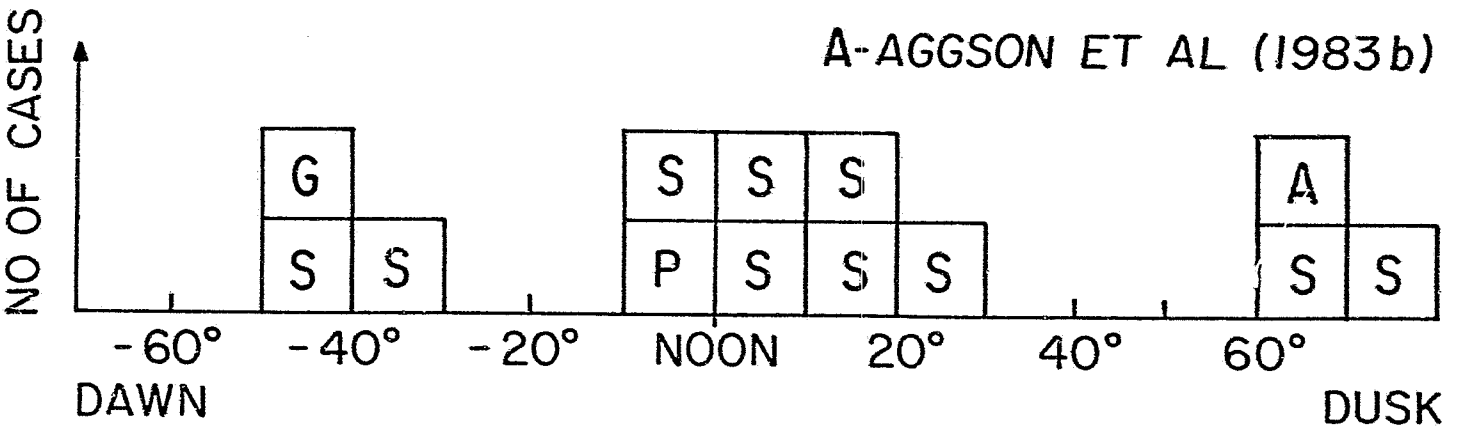

Figure 3

derived by Scudder and Aggson (1983). This bound equals 0.04 for $\psi = 175°$. These observed parameters suggest (at location of circled "x") that $\nu \backsim 0.4$ which corresponds very nearly to the observed deceleration of $\nu_{ob} = 130/300 \backsim .43$. The placement of this event in the framework of the present work represents a cross check since the current analysis is a generalization of Aggson's specific quadrature of (1). This analysis does indicate what parameters control the ν change across the RSL layer. An upper bound of the normal mass flux across the magnetopause can be made by virtue of the following identity:

$$n\, V_N \equiv n\gamma_*\, R_N\, V_T/R_T \backsim - n\, |\gamma_*|\, |\underline{V}^o|/R_T.$$

For the current parameters the normal mass flux of $\lesssim 6 \times 10^6/cm^2/s$ is inferred which corresponds to $V_N \lesssim 3$ km/s which is of course not directly measurable. This local rate of particle entry represents $\lesssim 1\%$ of the incident solar flux and is consistent with other (more global) estimates of the necessary solar wind replenishment of the plasma sheet given by Hill (1974) of 0.1-0.5%. These latter estimates are lower bounds for the efficiency of solar wind replenishment to the magnetosphere since they are determined on the basis of replenishing only the plasma sheet and not maintaining any other regions such as entry layers against their known losses.

A systematic survey of documented RSL's is required to further assess the concept that the magnetopause as a whole is globally open to directed normal mass flux. This possibility is certainly possible even with spatially localized separator lines as has been advocated, for example, by Crooker (1979). Such a survey must not select RSL event candiates based on parochial features of the Levy-Petschek-Siscoe normal incidence ($R_T = 0$) and maximum rotation ($\Delta\phi = \pi$) geometries such as speed increases or plasma jetting.

Acknowledgment

This work was motivated by a previous collaboration with T. Aggson on the interpretation of decelerating magnetopause rotational discontinuities and ongoing research with K. Ogilvie and C. T. Russell on flux transfer event

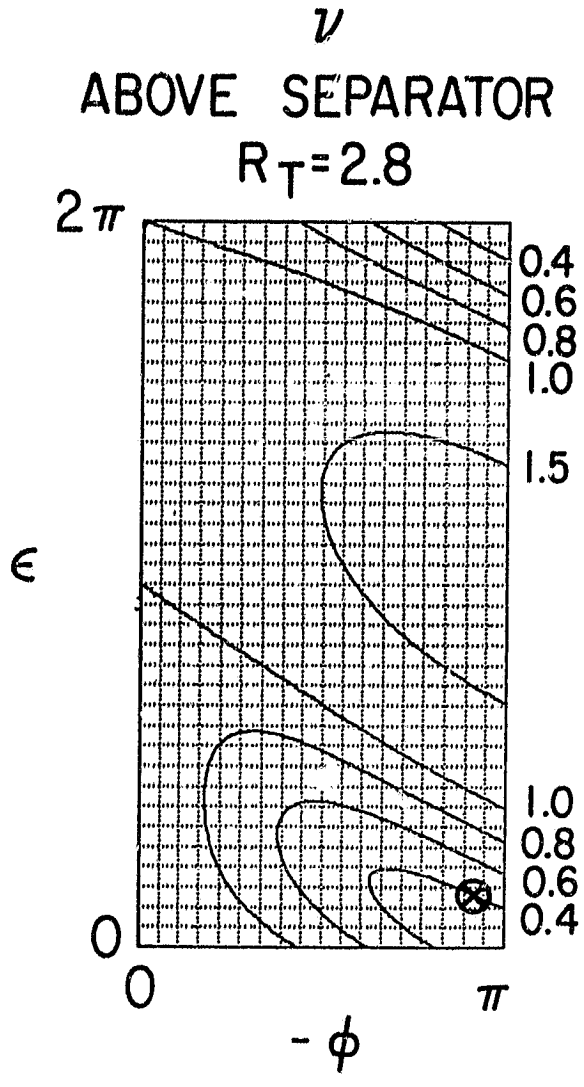

Figure 9

signatures. Manuscript comments by T. L. Aggson, L. F. Burlaga, D. H. Fairfield and A. Figueroa-Viñas are also acknowledged.

References

Aggson, T. L., P. J. Gambardella, and N. C. Maynard, "Electric Field Measurements at the Magnetopause: 1. Observation of Large Convective Velocities at Rotational Magnetopause Discontinuities," accepted J. Geophys. Res., 1983a.

Aggson, T. L., P. J. Gambardella, N. C. Maynard, K. W. Ogilvie and J. D. Scudder, "Observations of Plasma Deceleration at a Rotational Magnetopause Discontinuity," submitted Geophys. Res. Lett., 1983b.

Barnes, A. and J. V. Hollweg, "Large Amplitude Hydromagnetic Waves," J. Geophys. Res., 79, 2302, 1974.

Behannon, K. W. and L. F. Burlaga, "Alfvén Waves and Alfvénic Fluctuations in the Solar Wind," in Solar Wind Four, H. Rosenbauer, ed., p. 374, 1978, MPAE-W-100-81-31, Lindau, 1981.

Burlaga, L. F., J. F. Lemaire, and J. M. Turner, "Interplanetary Current Sheets," J. Geophys. Res., 82, 3191, 1977.

Crooker, N. U., "The Magnetospheric Boundary Layers: A Geometrically Explicit Model," J. Geophys. Res., 82, 3629, 1977.

DeHoffman, F. and E. Teller, "Magneto-Hydrodynamic Shocks," Phys. Rev., 80, 692, 1950.

Eastman, T. M. and E. W. Hones, Jr., "Characteristics of Magnetopause Boundary Layers as Observed by IMP 6," J. Geophys. Res., 84, 2019, 1979.

Gosling, J. T., J. R. Asbridge, S. J. Bame, W. C. Feldman, G. Paschmann, N. Sckopke, and C. T. Russell, "Evidence for Quasi-Stationary Reconnection at the Dayside Magnetopause," J. Geophys. Res., 87, 2147, 1982.

Goldstein, M. L., A. J. Klimas, and F. D. Barish, "On the Theory of Large Amplitude Alfvén Waves," Solar Wind Three, ed. C. T. Russell, 385, U. C. Press, Los Angeles, 1974.

Haerendel, G., G. Paschmann, N. Sckopke, H. Rosenbauer, and P. C. Hedgecock, "The Frontside Boundary Layer of the Magnetosphere and the problem of Reconnection," J. Geophys. Res., 83, 3195, 1978.

Heikkila, W. J., "Is There an Electrostatic Field Tangential to the Dayside Magnetopause and Neutral Line?", Geophys. Res. Lett., 2, 154, 1975.

Hill, T. W., Origin of the Plasma Sheet, Rev. Geophys. and Sp. Phys., 12, 379, 1974.

Levy, R. H., H. E. Petschek, and G. L. Siscoe, "Aerodynamic Aspects of Magnetospheric Flow," AIAA, 2, 2065, 1964.

Paschmann, G., B. U. O., Sonnerup, I. Papamastorakis, N. Sckopke, G. Haerendel, S. J. Bame, J. R. Asbridge, C. T. Russell, and R. C. Elphic, "Plasma Acceleration at the Earth's Magnetopause: Evidence for Reconnection," Nature, 282, 1979.

Paschmann, G., G. Haerendel, N. Sckopke, H. Rosenbauer, and P. C. Hedgecock, "Plasma and Magnetic Field Characteristics of the Distant Polar Cusp near Local Noon: The Entry Layer," J. Geophys. Res., 81, 2883, 1976.

Petschek, H. E., "The Mechanism for Reconnection of Geomagnetic and Interplanetary Field Lines," in The Solar Wind, R. J. Mackin and M. Neugebauer, eds. 257, Pergamon, New York, 1966.

Roederer, J. G., "Global Problems in Magnetospheric Plasma Physics and Prospects for their Solution, Space Sci. Rev., 21, 23, 1977.

Russell, C. T. and R. C. Elphic, ISEE Observations of Flux Transfer Events at the Dayside Magnetopause," Geophys. Res. Lett., 6, 33, 1979.

Scudder, J. D., K. W. Ogilvie and C. T. Russell, "The Electron Plasma Signatures of Flux Transfer Events": Evidence for Ongoing, Localized, Time Dependent Reconnection," to be submitted to J. Geophys. Res.

Scudder, J. D. and T. L. Aggson, "Analytical Bounds on the Normal Component at a Rotational Discontinuity in terms of Observables," to be submitted to J. Geophys. Res.

Sonnerup, B. U. O., and L. J. Cahill, Jr., "Explorer 12 Observations of the Magnetopause Current Layer," J. Geophys. Res., 73, 1757, 1968.

Sonnerup, B. U. O. and B. G. Ledley, "Magnetopause Rotational Forms," J. Geophys. Res., 79, 4309, 1974.

Sonnerup, B. U. O., and B. G. Ledley "Electromagnetic Structure of the Magnetopause and Boundary Layer" in Magnetospheric Boundary Layers, Proc. Chapman Conference, Alpbach Austria, June, 1979; ESA SP-148, P. 401, Noordwijk, Netherlands.

Sonnerup, B. U. O., G. Paschmann, I. Papmastroakis, N. Sckopke, G. Haerendel, S. J. Bame, J. R. Asbridge, J. T. Gosling, and C. T. Russell, "Evidence for Magnetic Field Reconnection at the Earth's Magnetopause," J. Geophys. Res., 86, 10,049, 1981.

Spreiter, J. R., A. L. Summers, A. Y. Alksne, "Hydromagnetic Flow Around the Magnetopause," Planet. Space Sci., 14, 223, 1966.

Walén, C., "On the Theory of Sunspots," Ark. f. Mat., Astr. o. Fysik, 30A, 15, 1944.

Whang, Y. C., "Alfvén Waves in Spiral Interplanetary Field," J. Geophys. Res., 78, 7221, 1973.

Figure Captions

Figure 1 — General geometrical construction of relationship of $\Delta\underline{V}_T$ to $\Delta\underline{\beta}_T$ appropriate for (electron polarization) Alfvén wave, rotational discontinuity (RD) or rotational shear layer (RSL). Where the arc A'C' (centered at 0) intersects semi-circle A'B'C'D' defines the minimum angle, ϕ^*, of magnetic rotation for the speed to have a net increase across the shear layer. Construction discussed extensively in the text. Note that $\underline{V}_T^o$ is related to the frame change velocity $\underline{U}^o$ used by de Hoffman and Teller (1950) by the relation $\underline{U}_o^{DHT} = \underline{V}_T^o - R_N \underline{\beta}_T^o = \underline{V}^o - R_N \underline{\beta}^o$, and corresponds to the vector from 0 to 0' which has been omitted for clarity.

Figure 2 — Petschek-Normal Incidence geometrical construction of Alfvén shear layer. Note that $V_T^o = 0$ and that $\Delta V(\phi) \equiv V_T(\phi)$ for all d. The "jetting" tendency is clarified by noting that

$$\lim_{\phi \to \pi} |\hat{V}_T(\phi) \cdot \hat{\beta}_T(\phi)| \to +1.$$

Figure 3 — Geometry of RSL below (a) and above (b) the separator (electron polarization) standing in the flow as appropriate at the magnetopause. Notice that if electron polarization is assumed that the sign of $\dot{\phi}$ implies location of observations re separator since $R_N \equiv -\dot{\phi}/|\dot{\phi}|$.

Figure 4 — Graphical survey of scaled speed ν, as determined from equation 4 for fixed constant normal mass flow, γ^*, R_N^*, but considering the spectrum of possibilities as a function of R_T (rows of boxes), as a function of below (a) or above (b) the separator as a function of the incident flow-field geometry, ε, and the magnitude of the angle of magnetic rotations, ϕ. Dynamo regimes correspond to $\nu < 1$ contours.

Figure 5 — Synthesis of $\nu = 1$ contours of Figure 4A-F in 5a (below) and Figures 4C-L in 5b above the separator. Contours are labeled according to R_T regime and are loci of $\nu = 1$. Notice by definition that the left vertical axis is always an isocontour for any R_T. Dynamo regions in (a) are bounded by left vertical axis and contours labeled according to value of R_T. Dynamo regions in 5(b) are similar to those in 5a except that these regimes are disjoint; region above "motor only" are inside domains defined by the right vertical axis, top horizontal axis and contour curves. Motor regimes for specified R_T. Shaded regions denoted "motor-only" cannot have dynamo layers for any value of R_T. See analysis starting with equation 10. Dashed lines reflect the theoretical bound of the motor only regimes as derived in the text.

Figure 6 — Survey in the format of Figure 4 of the generality of "jetting" $\delta = \sphericalangle \vec{V}, \vec{B} \simeq 0, \pi$ and "convection" $\delta \simeq \pi/2$. Notice that "jetting" will not be a general property for resolved layers or very thin layers with $\phi < \pi$, or for general Mach numbers (cf. e.g., $R_T = 10$).

Figure 7 — Tangential Mach number, R_T, distribution of extant RSL layers reported to date. Note that speed increasing layers $\nu > 1$ are localized below unity, whereas the decelerating observation was observed for large R_T of 2.8. Compare with patterns expected in Figure 4 for R_T dependence with other things being equal.

Figure 8 — Subsolar angular distribution of events in Figure 7.

Figure 9 — Isocontours of ν for $R_T = 2.8$ above separator, $R_N = +1$, and $\gamma^{-1} = B_T/B_N = -20\sqrt{2}$ chosen for comparison with Aggson et al. (1983b), $\nu < 1$ event. Circled x is the location of $-\Delta\phi = 165$, $\varepsilon = 25°$ appropriate to geometrical (boundary) conditions of observation.